Atmos. Chem. Phys. Discuss., 8, 4117–4154, 2008
www.atmos-chem-phys-discuss.net/8/4117/2008/

Atmospheric Chemistry and Physics Discussions

Lagrangian transport modelling for CO_2 using two different biosphere models

G. Pieterse[1,2], **A. T. Vermeulen**[1], **I. T. Baker**[3], **and A. S. Denning**[3]

[1]Energy research Centre of the Netherlands, Petten, The Netherlands
[2]Institute for Marine and Atmospheric Research Utrecht, Utrecht, The Netherlands
[3]Colorado State University, Fort Collins, USA

Received: 4 December 2007 – Accepted: 11 January 2008 – Published: 28 February 2008

Correspondence to: G. Pieterse (gerben_pieterse@hotmail.com)

Abstract

In this work, the performance of the Framework for Atmosphere-Canopy Exchange Modelling (FACEM: Pieterse et al., 2007) coupled to a Lagrangian atmospheric transport model is evaluated for carbon dioxide. Before incorporating FACEM into the Lagrangian COMET model (Vermeulen et al., 2006), its performance for the European domain is compared with the Simple Biosphere model (SiB3: Sellers et al., 1996). Overall, FACEM is well correlated to SiB3 ($R^2 \geq 0.60$), but shows less variability for regions with predominantly bare soil. There is no significant overall bias between the models except for the winter conditions and in general for the Iberian peninsula. When coupled to the COMET transport model, both biosphere models yield similar correlations ($R^2 \geq 0.60$) and bias relative to the 1-hourly concentration measurements for the year 2002, performed at three different sites in Europe; Cabauw (Netherlands), Hegyhatsal (Hungary) and Mace Head (Ireland). The overall results indicate that FACEM is comparable to SiB3 in terms of its applicability for atmospheric modelling studies.

1 Introduction

A significant part of the work performed within the field of environmental research is currently focussing on the development of climate models (Randall et al., 2007). The goal of the scientific work on this subject is to produce realistic predictions for the short and long term response of the global climate system on the increasing carbon dioxide concentration (IPCC, 2007). The most challenging part is that a large number of physical, chemical and/or biological processes occurring over a large range of temporal and spatial scales have a significant effect and therefore must be incorporated in these models for adequate predictions.

Of high importance is an appropriate scheme that describes the short and long term biospheric response to climatic drivers such as solar radiation, precipitation, air temperature, CO_2, and others. The implementation of such a scheme requires sound

insight into the spatial and temporal impact of the main processes determining the magnitude and timing of the response of the terrestrial biosphere to the main driving parameters. For this purpose, numerous advanced physiological, flux and concentration measurements (laboratory scale, ground based, airborne or remote sensing), are currently performed or developed. Realisation of such measurements is still accompanied with technological and methodological challenges, of which accuracy, precision and inter comparability are the most important limiting factors.

During the last 30 years a world wide network of measurement sites has been established to monitor the global trend of CO_2 and other greenhouse gases (Globalview-CO_2, 2005). The sites contributing to this network are located at remote regions to reduce the local influence of anthropogenic and biogenic contributions compared to the much slower varying global background concentrations. Highly accurate calibration methods and data qualification routines are used to ensure optimal data quality (World Meteorological Organisation, 2007). These procedures make the data obtained from these sites very valuable for longer term global climate studies. However, these measurements are by design less suitable for continental greenhouse budget investigations as the source and sink information is too diluted at these sites. Therefore, recent projects, e.g. CarboEurope IP (http://www.carboeurope.org), the project for Continuous HIgh-precisiOn Tall Tower Observations (CHIOTTO: http://www.chiotto.org), and the North American Carbon Program (NACP: http://www.nacarbon.org/nacp), have focussed on developing networks of continental sites employed especially to monitor continental CO_2 concentrations. These sites are generally situated in regions highly influenced by anthropogenic as well as biospheric activity. Hence, the measurements obtained from these sites are complex mixed signals with large and (sometimes) compensating contributions from biospheric and anthropogenic activity. Adequately interpreting these signals and quantifying the biospheric and anthropogenic contributions to these signals requires the use of accurate high resolution atmospheric transport models.

However, it is this same complexity that renders evaluation of the performance of

such atmospheric transport models difficult. This asks for the concurrent development of sophisticated biosphere models that are able to accurately describe the processes that take place in the biosphere. The approach that is chosen for this study however is partly moving away from this growing complexity for reasons explained below.

An important fact is that most biospheric and atmospheric model studies are almost by definition under determined, i.e. that there are not enough measurements available to solve for all unknowns in a certain problem. As a general rule, a certain minimum number of processes that capture the most important features of a certain complex system need to be included in a model. Adding more processes in an attempt to capture even more features does not necessarily lead to improved accuracy, even though these newly added processes can be conceptually correct and their inclusion seems justifiable. Namely, along with each new process, a number of new parameters are introduced. An increasing amount of poorly determined parameters will add to the uncertainty and it is therefore important to realise that including more complexity can lead to loss of accuracy.

This work illustrates the applicability of a new biosphere model, the Framework for Atmosphere Canopy Exchange Modelling (FACEM: Pieterse et al., 2007), to atmospheric transport modelling of CO_2. For this purpose, FACEM was coupled to the Lagrangian CO_2 and Methane Transport (COMET) model (Vermeulen et al., 1999, 2006). Both models were developed keeping the above described “uncertainty accumulation” in mind and only contain the crucial processes required to capture the most important features of atmospheric transport and the biospheric processes responsible for the exchange of CO_2 between the biosphere and atmosphere. This design limits the application of both models to regions without complex orographic features. Section 2 starts with a brief description of the overall model framework and the chosen method of evaluation. The results are described in Sect. 3 and summarised in Sect. 4.

2 Methods

Before addressing the full model framework, the model is evaluated by a European scale comparison between FACEM and the more sophisticated Simple Biosphere model (SiB: Sellers et al., 1996) that provides global biospheric CO_2 flux estimates. Thereafter, both biosphere models are coupled to COMET and the overall performance is evaluated in a comparison with 1-hourly concentration measurements from three different European continuous measurement sites for the year 2002. Both model frameworks are evaluated with respect to their capability to predict the concentrations measured at these sites.

2.1 Used models and additional data

2.1.1 Biosphere models

FACEM is a Soil-Vegetation-Atmosphere-Transfer (SVAT) model that calculates Gross Primary Productivity (GPP), Net Primary Productivity (NPP) and Net Ecosystem Productivity (NEP). The GPP accounts only for the uptake of CO_2 due to photosynthesis. NPP also incorporates the release of CO_2 due to biomass growth and maintenance (i.e. autotrophic respiration). NEP accounts for all processes including the release of CO_2 from the soil carbon pools due to microbe activity (i.e. heterotrophic respiration). The sum of autotrophic and heterotrophic respiration is called total respiration. With FACEM, these quantities can be calculated on a 1-hourly time resolution and a spatial resolution of $0.5^\circ \times 0.5^\circ$ for the European domain.

Within FACEM, the exchange of CO_2 between the biosphere and the atmosphere is modelled using a mechanical multi layer model for photosynthesis (Berry and Farquhar, 1978; Collatz et al., 1991; Wu et al., 2003). A passive membrane transport model is used to calculate the leaf cuticle resistance. The photosynthesis scheme provides a full description of the stomatal resistance of the leafs coupled to the biochemical mechanisms governing photosynthesis and also considers the (coupled) effects of environ-

mental conditions. Compared to the traditional single layer approach, the multi layer approach allows for a more adequate treatment of the non-linear transport of radiation through the canopy and a more accurate calculation of the boundary layer resistance. Autotrophic respiration is estimated by a scheme adopted from an algorithm used to produce MODIS NPP products (Heinsch et al., 2003). Growth respiration is calculated following the approach introduced by Knorr (2000). Finally, heterotrophic respiration is calculated using the approach introduced by Ito and Oikawa (2000) and Aurora (2003). A more detailed description of FACEM was previously given by Pieterse et al. (2007).

The SiB model was described extensively in (Sellers et al., 1996; Denning et al., 1996; Baker et al., 2003; Vidale and Stoekli, 2005; Baker et al., 2006) and yields global 1-hourly fluxes for GPP and total respiration on a $1.0^\circ \times 1.0^\circ$ resolution (Baker et al., 2007). Conceptually, FACEM and SiB differ significantly. FACEM was mainly designed for provision of reasonable initial estimates for forward and inverse modelling of the current exchange of CO_2 between the biosphere and atmosphere and makes use of available measurements whenever the alternative, a mechanical model, is considered to be a source of larger uncertainty. SiB was originally designed for calculating the exchange of energy, mass and momentum from the terrestrial biosphere to the lower boundary of atmospheric circulation models. For this purpose and to address also more detailed ecological questions, inclusion of the exchange of CO_2 between the biosphere and atmosphere was vital. Because CO_2 is an important driver for global climate (IPCC, 2007), it is important to keep track of the present, past and future carbon budgets for the atmosphere, vegetation as well as for the soil. Since more and more measurements have become available recently, the latest versions of the SiB model (resulting in SiB3) have been optimised in its ability to reproduce these measurements. It is for this reason that the SiB3 model is considered an excellent benchmark to validate FACEM.

2.2 Atmospheric transport model

A detailed theoretical treatment and validation of the Lagrangian CO_2 and Methane Transport (COMET) model was previously given by Vermeulen et al. (1999, 2006). In short, the COMET model approximates the transport of any chemically inert gaseous atmospheric constituent towards a measurement site by a closed 2-layer box moving along a Lagrangian trajectory that ends at the measurement site. The trajectories are obtained using the Flextra model (Stohl et al., 1995; Stohl and Seibert, 1998) which uses the same European Centre of Medium range Weather Forecast (ECMWF) data that is used by the FACEM model. While moving along the trajectory, the box accumulates and releases tracer, in this case CO_2, from and to the surface sources and sinks. The height of the interface between the two layers in the box changes according to the calculated Planetary Boundary Layer (PBL) height. This models the exchange of air between the lower well-mixed and the upper reservoir layer. By initialising the concentrations at the start of each trajectory to the spatially interpolated background concentration measurement data provided by Globalview-CO_2 (Globalview-CO_2, 2005), and by employing the estimates for the spatial and temporal distribution of sources and sinks for CO_2, the COMET model provides means to calculate 1-hourly averaged CO_2 concentrations for any given measurement site within the well-mixed PBL. The results shown in this paper will focus on the domain of western Europe.

2.3 Used additional data sets

A global data set (Takahashi et al., 2002) was used to provide estimates for the exchange of carbon dioxide between the atmosphere and the ocean. Finally, the Edgar Fast Track emission inventory (Olivier et al., 2005) was used to provide the anthropogenic emission estimates.

3 Model evaluation

In this section, FACEM and SiB3 are first compared for the European domain. Thereafter, both models are coupled to COMET and the resulting modelled well-mixed layer concentrations are compared to the measurements at Cabauw, Hegygatsal and Mace Head.

3.1 Flux model evaluation

The grid based evaluation described in this section required spatial matching of the results because FACEM and SiB3 are run at different spatial resolutions (see Sect. 2.1.1) and by default use different land masks. Therefore, the land mask of the SiB3 model was applied to the FACEM model results after completing the calculations using the FACEM land mask. Grid cells for which model results were available from only one of the two models, were excluded. SiB3 provides results for GPP and total respiration. Therefore, we chose to compare GPP and NEP.

3.1.1 Gross Primary Productivity

In Fig. 1, the spatial correlation (R^2) between the modelled GPP fluxes, the relative difference in the standard deviation ($\Delta\sigma$) and relative bias between the modelled GPP fluxes are shown for the spring (a–c), summer (d–f), autumn (g–i) and winter (j–l) season. The latter two quantities are referenced to the SiB3 model results and are expressed in relative deviation percentages.

It is clear that both models correlate well ($R^2 \geq 0.60$) for the spring season, except for the Northern part of Scandinavia and for the Iberian peninsula. For high latitudes, the Leaf Area Index (LAI) product (Knyazikhin et al., 1999) used by FACEM is scarce and less accurate. For these regions, this could well be an explanation for the discrepancy between both models. In the central part of the Iberian peninsula GPP is low and therefore small differences between both models have a large effect on correlation and

relative differences between variability and bias. This is also the case for the winter season when GPP is low all over Europe. Additionally, the land use classes for the Iberian peninsula are different for both models. FACEM assigns C3 crops and grasses to this region whereas SiB3 uses broad leaf deciduous trees over wheat. The use of different land use classes is very likely the cause for the observed differences between the model results for the Iberian Peninsula.

For the United Kingdom, FACEM yields significantly less variable and lower average GPP. FACEM uses interpolated meteorological data to calculate the fluxes at a resolution of $0.5^{\circ}\times0.5^{\circ}$. The SiB3 calculations were performed at a coarser spatial resolution and the fluxes are provided at a resolution of $1.0^{\circ}\times1.0^{\circ}$. This difference can cause significant differences for locations with mixed oceanic and continental meteorological conditions, e.g. the United Kingdom or Ireland. Section 3.2.3 will discuss this phenomenon in a comparison with measurements performed at the Mace Head station.

In all, the two models correlate reasonably well ($R^2 \geq 0.50$) for the Summer season, with again the exception of the Iberian peninsula. An anomaly of enhanced variability and positive bias occurs in the Southern part of France during Summer and Autumn. The Available Soil Water (ASW) budget implemented in FACEM indicates a relatively high ASW content for this region but the ASW is still in the optimal range for photosynthesis. In Fig. 2, the seasonally averaged results of both models are compared with the seasonally averaged MODIS GPP product (Heinsch et al., 2003). For the spring, summer and autumn season both FACEM and MODIS show enhanced GPP for the Southern part of France. It is clear that, overall, FACEM and the MODIS produce very similar spatial patterns. This not surprising because FACEM makes use of the MODIS LAI product to calculate GPP whereas in SiB3 Normalised Difference Vegetation Index (NVDI) data from the Advanced Very High Resolution Radiometer (AVHRR: Teillet et al., 2000) is used. It is therefore likely that the differences between both models can be explained by the different distributions of LAI derived from the observations.

3.1.2 Net Ecosystem Productivity

Figure 3 shows the correlation (R^2), relative difference in the standard deviation ($\Delta\sigma$) and the relative bias between the modelled NEP fluxes for the spring (a–c), summer (d–f), autumn (g–i) and winter (j–l) season. Again, the latter two quantities are referenced to the SiB3 model results and are expressed in deviation percentages.

The figure shows similar but more pronounced discrepancies as those found for the GPP fluxes in the previous section. The differences are again largest for the Iberian peninsula, the higher latitudes and the United Kingdom. In the North-Eastern part of Europe the average NEP, as predicted by FACEM, is larger by more than 80%. In the current version of FACEM, the autotrophic respiration model does not account for snow cover or frost conditions. Adapting the soil respiration scheme in FACEM for winter conditions will most likely improve the performance. Furthermore, SiB3 is well equipped for predicting the diurnal and seasonal variability but is not designed to reproduce net sources and sinks. The magnitude of a net local source or sink at a certain location is small, generally in the order of 10% or less. An uncertainty in the magnitude of this local source or sink will therefore not significantly affect the absolute error in the calculated instantaneous flux (Denning et al., 1996). Therefore, SiB3 forces annual NEP to zero and the respiration fluxes will on average exactly cancel the GPP fluxes. Both models agree well for the central part of Europe, which is the region of interest for the comparison in the following section.

3.2 Overall model evaluation

COMET model calculations were performed for the Cabauw tall tower site (Ulden and Wieringa, 1996; Beljaars and Bosveld, 1997) in the Netherlands and the results were compared with 1-hourly averaged PBL concentration measurements for the year 2002. The following six cases were considered for the evaluation:

Case 4 and 6 were also investigated for the daytime (09:00 a.m.–06:00 p.m.) and nighttime results. These cases allows for subsequent validation of the schemes for

photosynthesis or primary productivity (case 2 and 5), autotrophic respiration (added in case 3) and heterotrophic respiration (added in case 4 and 6). Case 1 is the reference case and gives insight in the magnitude of the contributions from anthropogenic sources and oceanic sinks, the latter of which was considered small compared to the anthropogenic contributions. The same procedure was repeated for the Hegyhatsal Tall tower in Hungary (Hazpra, 2006) and the Mace Head observatory in Ireland (Derwent et al., 2002), also for the year 2002. The three sites are described in Table 2.

3.2.1 The Cabauw tall tower

For the Cabauw tall tower, the results for the different cases are shown in Table 3.

The results clearly indicate that incorporating the NEP as an estimate for the biosphere-atmosphere exchange yields the best model-to-measurement correspondence, both in terms of correlation as well as in terms of variability and bias. This is valid for both FACEM as well as SIB3 and indicates good performance of all processes included in the FACEM and the SiB3 model, especially considering the completely different agreement for Case 2, measured by a poor correlation (R^2=0.35). Overall, the performance obtained using FACEM is comparable to the performance obtained using SiB3, also for day and night time conditions. In Fig. 4, the monthly averaged diurnal cycles of the modelled and measured signals are shown. All months have ≥75% valid data coverage except January (45%), April (9%), May (54%), August (64%) and December (0%).

The anthropogenic and oceanic contributions (solid red) add relatively little to the variability of the modelled signals, suggesting a larger influence of the local terrestrial biosphere on the measured variability than the local anthropogenic sources. For both biosphere models, GPP is responsible for a large uptake of CO_2 (solid and dashed green) during the spring and summer season. However, this uptake is compensated by release of CO_2 due to autotrophic and heterotrophic respiration, as illustrated by the yellow, solid blue and dashed blue lines. As it should be, including all important emissions and uptakes (solid and dashed blue lines) leads to the best model-

to-measurement performance. For the winter months, when respiration processes dominate the biospheric flux, the variability is well predicted by both biosphere models, however the model results show a stronger bias. As mentioned in Sect. 2.2, the transport model is initialised by measured background concentrations. An important limitation of this approach is that for cases where the used background concentration (at the starting point of each trajectory) is not representative for the actual background concentration, a bias will be observed between the modelled and measured concentrations leading to lower modelled concentrations compared to the observed concentrations. Such circumstances develop mainly in the winter season with flow conditions where continental air masses are transported from east to west, which is the case for Cabauw.

It is striking to see how the modelled GPP signal is concealed by heterotrophic respiration. The uptakes of CO_2 due to photosynthesis, that are clearly present in case 2 and 5 are barely discernible in the measured signals. This has an important consequence for the use of concentration measurements for estimating the carbon budget in the influence area of this measurement site. It will be difficult, if not impossible, to dissect the different contributions of the biosphere to the measurements using concentration measurements only. Considering the magnitude of the contributing and opposing signals and the uncertainties involved in the atmospheric transport modelling, determining the different contributions would very likely result in significant uncertainties. However, it appears that determining the combined contributions of the anthropogenic sources and NEP is feasible, considering the good model-to-measurement correspondence represented by cases 4 and 6.

3.2.2 The Hegyhatsal tall tower

For the Hegyhatsal tall tower, the results for the different cases are shown in Table 4.

A striking difference with the model performance for Cabauw can be seen here for case 1. As the activity of fossil fuel sources around the Hegyhatsal site is very low compared to the Cabauw site, there is no correlation between the model and measure-

ments for the case when only fossil fuel sources are taken into account. Again, the NEP case results in the best model-to-measurement correspondence, both in terms of correlation as well as in variability and bias. In Fig. 5, the monthly averaged diurnal cycles of the modelled and measured signals are shown. All months have ≥75% valid data coverage except January (0%), July (65%), August (14%) and September (41%).

From this figure, it can be seen that the contribution of fossil fuel emissions to the diurnal cycle are nearly negligible (red). The GPP (solid and dashed green) is clearly responsible for a large uptake of CO_2 during spring and summer. Again, this uptake is compensated by releases due to autotrophic and heterotrophic respiration (orange, solid and dashed blue). The model results using NEP fluxes from SiB3 (dashed blue) overestimate the measurements. Assuming that SiB3 fluxes are correct, this leads to the conclusion that the nocturnal PBL height is underestimated for stable night time conditions. In the PBL scheme implemented in COMET, the PBL height is limited to a minimum height of 50m. It is plausible that more vertical mixing occurs due to local surface inhomogeneities than is predicted using the relatively coarse ECMWF data. For this reason, the COMET model calculations were repeated using the SiB3 NEP estimates and using 100m as the lower limit for the nocturnal PBL height, resulting in a significant improvement (R^2=0.55, σ=13.2 ppm, bias=–2.2 ppm) compared to Case 6 in Table 4 (R^2=0.44, σ=23.1 ppm, bias=3.5 ppm). It is also possible that the modelled heterotrophic respiration fluxes from SiB3 are too large for the region of influence of the Hegyhatsal tower. As can be seen in Fig. 2, SiB3 tends to predict larger GPP in Hungary than observed by MODIS, and therefore the heterotrophic respiration fluxes are expected to be relatively high as well (see Sect. 3.1.2. CO_2 flux measurements are required to determine whether (a combination of) both sources of error can explain the discrepancy but were not available for this study.

3.2.3 The Mace Head site

For the site at Mace Head, the results for the different cases are summarised in Table 5.

Again, the NEP case results in the best model-to-measurement correspondence,

both in terms of correlation as well as in bias. Figure 6 shows the monthly averaged diurnal cycles of the modelled and measured signals. All months have ≥75% valid data coverage except July (16%) and August (59%).

The Mace Head station is used for the purpose of obtaining boundary condition measurements for the European domain. Figure 6 shows that the anthropogenic contribution is indeed low (red). Larger uptakes of CO_2 (dashed and solid green) are observed during periods with winds from easterly directions when the Irish and UK islands and the European continent are within the region of influence. These uptakes are again compensated by autotrophic and heterotrophic respiration (yellow, dashed and solid blue). The night time variability is overestimated when using the SiB3 NEP fluxes (σ=10.2 ppm instead of 5.8 ppm). By setting the lower limit for the PBL height to 100 m instead of 50 m the performance (R^2=0.46, σ=6.6 ppm, bias=–1.4 ppm) improves compared to Case 6 in Table 5 (R^2=0.27, σ=10.2 ppm, bias=–1.8 ppm). However, as was the case for the Hegyhatsal site in the previous section, the correlation does not improve to the same value as obtained using the FACEM model output. Furthermore, as can be seen in Fig. 2, SiB3 tends to predict larger GPP in Ireland than observed by MODIS, and therefore the heterotrophic respiration fluxes are expected to be relatively high as well (see Sect. 3.1.2. We also expect that the differences can be caused by the different spatial resolutions of the two biosphere models; The FACEM fluxes are available at twice the resolution as the SiB3 fluxes. Mace Head is located at 9.54° W, which is rather close to the border of two adjacent grid-cells and located in the coastal region of Ireland. Falsely attributing terrestrial fluxes to a station with a predominantly marine region of influence can result in over estimation of variability. Indeed, the performance compared to Case 6 in Table 5 shows further improvement after shifting the SiB3 fluxes one grid-cell further east (R^2=0.51, σ=5.3 ppm, bias=–2.3 ppm). This improvement suggests that one can considerably improve the modelled concentrations for stations that are known to be near to sharp boundaries between different biomes by either using higher resolution model data or interpolated coarser resolution data.

4 Conclusions

4.1 Flux model evaluation

The FACEM and SiB3 GPP fluxes indicate similar behaviour of both biosphere models for the central part of Europe, measured by good spatial correlations ($R^2 \geq 0.60$), reasonable differences in variability ($|\Delta\sigma| \leq 40\%$) and a small bias ($\leq 40\%$) for most regions. For high latitudes, the availability of accurate LAI data is a limiting factor, especially for the winter season. We expect that implementation of fixed low-values LAI estimates for these region will improve the performance of FACEM for the winter season.

Both models yield significantly different GPP for the Southern part of France. We suggest that these differences are caused by the different spatial distributions of LAI that are used to calculate GPP; SiB3 and FACEM use the observations of different satellite platforms to derive this important parameter. For regions with mixed oceanic and continental meteorological conditions, such as Ireland and the United Kingdom, the different spatial resolutions of FACEM and SiB3 ($0.5^\circ \times 0.5^\circ$ and $1.0^\circ \times 1.0^\circ$, respectively) differences were also expected and observed; FACEM predicts up to 40% less variability in GPP and 40% lower average productivity than SiB3. Section 4.2 will elaborate more on this subject.

For NEP, similar but more pronounced discrepancies were observed between FACEM and SiB3 model results. Furthermore, FACEM predicts a much larger NEP for the winter season. This difference can be explained by the fact that the heterotrophic respiration scheme implemented in FACEM does not account for snow cover and frost conditions. It is expected that incorporating such a dependency will result in more representative NEP fluxes for the winter season in the FACEM model.

4.2 Overall model evaluation

The results presented in Sect. 3.2 show that the combined model framework, i.e. the flux models combined with the Lagrangian transport model COMET, is capable of re-

producing the measurements of three different sites in the European domain well. Daytime concentrations were modelled with convincing correlations (R^2=0.62–0.75). The night-time predicted concentrations showed less correlation (R^2=0.46–0.57). An important factor influencing the absolute night time concentrations is the height of the nocturnal PBL. Model results obtained using SiB3 NEP fluxes frequently overestimated night time concentrations for the Hegyhatsal tall tower and the Mace Head station. In the BPL scheme that is implemented in COMET the stable PBL height was limited to a minimum of 50 m. Increasing this lower limit to a value of 100 m and repeating the calculations for SiB3 improved the night-time performance significantly. For Hegyhatsal, the performance improved from R^2=0.44, σ=23.1 ppm and bias=3.5 ppm to R^2=0.55, σ=13.2 ppm and bias=–2.2 ppm. For Mace Head, the performance also improved, from R^2=0.27, σ=10.2 ppm and bias=–1.8 ppm to R^2=0.46, σ=6.6 ppm and bias=–1.4 ppm. However, this did not lead to similar performance as observed when the FACEM NEP fluxes were used. It is likely that this difference can be explained by the different spatial resolutions of both biosphere models. Especially for sites located near boundaries between oceanic and continental grid cells, such as Mace Head, using biosphere models with different spatial resolution will lead to significantly different results. Indeed, the results showed further improvement after shifting the SiB3 NEP fluxes one grid-cell further east (R^2=0.51, σ=5.3 ppm, bias=–2.3 ppm), herewith increasing the influence of the oceanic fluxes compared to the fluxes of the terrestrial biosphere. The difference in performance could also be explained by the different approaches followed to calculate NEP. The annual NEP is constrained to zero in SiB3, whereas soil carbon pools are used to calculate heterotrophic respiration in FACEM. For regions with larger modelled GPP fluxes, SiB3 will on average also predict larger heterotrophic respiration fluxes. This can result in over predictions in modelled night-time PBL concentrations when photosynthesis does not contribute.

This work also illustrates the limitations for possible extraction of the biospheric and anthropogenic contributions to atmospheric concentration measurements. The GPP signal is difficult to discern in the measured concentrations of the three sites considered

in this study. The sites are typical continuous (tall tower) sites and representative for other sites over the globe. Mace Head is situated in a remote location barely influenced by biospheric and anthropogenic activity. Cabauw is situated in a region with high anthropogenic activity and Hegyhatsal in a region with predominantly biogenic activity. We therefore expect that it will be difficult, if not impossible, to extract the GPP signal directly from atmospheric concentration measurements alone. This problem is mainly caused by well-mixed state of the planetary boundary layer during day time, resulting in significant dilution of GPP information present in the measured signals. Additional flux measurements could provide better means to separate the signals of the different parts of the biosphere. Measurements obtained from locations with less pronounced human contributions will allow for a better opportunity to derive the GPP signal. Additional tracers could be very useful to separate the signal due to anthropogenic emissions from the biospheric fluxes. A possibility is the use of $^{14}CO_2$ measurements (IPCC, 2007), with the disadvantage of the more expensive measurement techniques involved and the low temporal resolution of such measurements. CO measurements do not have this disadvantage, but the CO-to-CO_2 ratios for the different fossil fuel sources have a rather wide range (Levin and Kastens, 2007) and direct comparison of these two tracers is therefore limited. Another possibility would be the use of CH_4 concentrations as a proxy for human emissions, but here the disadvantage is that the co-location between anthropogenic CO_2 and CH_4 sources is far from ideal and that major natural sources of CH_4 that are not associated with CO_2 emissions also exist.

The human emissions of CO_2 are known quite accurately. A more promising approach would be to subtract the modelled concentration signals due to anthropogenic emissions from the measured signal followed by a partitioning of the remaining signal between GPP and respiration. During night time, the signal is clearly dominated by respiration processes and the measurements seem to provide much information about these processes. Possibly, estimates for night time respiration can be derived from the night time concentration measurements, provided that accurate estimates for the anthropogenic sources and an adequate description of atmospheric transport are

available. However, night time conditions are currently still hard to reproduce by atmospheric transport models and uncertainties introduced by these models will limit accurate footprint analysis for nighttime concentrations. Therefore, quantifying the impact of the biosphere on the carbon budget, based on concentration measurements, is expected to remain a tough problem to tackle in the near future.

Acknowledgements. We would like to acknowledge the World Data Centre for Greenhouse Gases (WDCGG), the CarboEurope project and Aerocarb project for providing the CO_2 concentration measurements required for the model-to-measurement comparisons. Also, we would like to thank T. Röckmann from the Institute for Marine and Atmospheric research in Utrecht (IMAU) in the Netherlands for his valuable comments on this manuscript.

References

Aurora, V. K.: Simulating energy and carbon fluxes over winter wheat using coupled land surface and terrestrial models, Agr. Forest Meteorol., 118, 21–47, 2003. 4122

Baker, I. T., Denning, A. S., Hanan, N. P., Prihodko, L., Uliasz, M., Vidale, P.-L., Davis, K., and Bakwin, P.: Simulated and observed fluxes of sensible and latent heat and CO_2 at the WLEF-TV tower using SiB2.5, Glob. Change. Biol., 9, 1262-1277, 2003. 4122

Baker, I. T., Denning, A. S., Hanan, H., Berry, J. A., Collatz, G. J., et al.: The next generation of the simple biosphere model (SiB3): model formulation and preliminary results, in: Proceedings of the 1st iLEAPs Science Conference, edited by: Reissell, A. and Aarflot, A., Finish Association for Aerosol Research, Boulder, Colorado, USA, 2006. 4122

Baker, I. T., Berry, J. A., Collatz, G. J., Denning, A. S., Hanan, N. P., Philpott, A. W., Prihodko, L., Schaefer, K. M., Stockli, R. S., and Suits, N. S.: Global net ecosystem exchange NEE fluxes of CO_2, Available online [http://www.daac.ornl.gov] from ORNL Distributed Active Archive Center, Oak Ridge, USA, 2007. 4122

Beljaars, A. C. M. and Bosveld, F. C.: Cabauw data for the validation of land surface parameterization schemes, J. Climate, 10(6), 1172–1193, 1997. 4126

Berry, J. A. and Farquhar, G. D. (1978). The CO_2 concentration function of C_4 photo synthesis: A biochemical model, in: 4th International Congress of Photosynthesis, edied by: Jall, D., Coombs, J., and Goodwin, T.,119–131, London, Biochem. Soc., 1978. 4121

Collatz, G. J., Ball, K. T., Grivet, C., and Berry, J. A.: Physiological and environental regulation of stomatal conductance, photo synthesis and transpiration: A model that includes a laminar boundary layer, Agr. Forest Meteorol., 54, 107–136, 1991. 4121

Denning, A. S., Collatz, G. J., Zhang, C., Randall, D. A., Berry, J. A., Sellers, P. J., Colello, G. D., and Dazlich, D. A.: Simulations of terrestrial carbon metabolism and atmospheric CO_2 in a general circulation model. part 1: Surface carbon fluxes, Tellus, 48B, 521–542, 1996. 4122, 4126

Derwent, R. G., Ryall, D. B., Manning, A. J., Simmonds, P. G., O'Doherty, S., Biraud, S., Ciais, P., M., R., and Jennings, S. G. : Continuous observations of carbon dioxide at mace head, ireland from 1995 to 1999 and its net european ecosystem exchange, Atmos. Environ., 36(17), 2799–2807, 2002. 4127

Globalview-CO_2: Cooperative Atmospheric Data Integration Project – Carbon Dioxide, 2005. 4119, 4123

Hazpra, L.: Atmospheric CO_2 hourly concentration data, hegyhatsal (HUN), World Data Centre for Greenhouse Gases, Japan Meteorological Agency, 20 Tokyo, available at: http://gaw.kishou.go.jp/wdcgg.html, 2006. 4127

Heinsch, F. A., Reeves, M., Bowker, C. F., Votava, P., Kang, S., Milesi, C., Zhao, M., Glassy, J., Jolly, W. M., Kimball, J. S., Nemani, R. R., and Running, S. W.: Users guide: GPP and NPP (MOD17A2/A3) products NASA MODIS land algorithm, 2003. 4122, 4125

IPCC: Climate change 2007: The physical science basis. contribution of working group I to the fourth assessment report of the intergovernmental panel on climate change, in: Fourth IPCC Assessment Report, edited by: Solomon, S., Qin, D., Manning, M., Chen, Z., Marquis, M., Averyt, K., Tignor, M., and Miller, H., Cambridge University Press, Cambridge, United Kingdom and New York, 2007. 4118, 4122, 4133

Ito, A. and Oikawa, T.: A model analysis of the relationship between climate perturbations and carbon budget anomalies in global terrestrial ecosystems: 1970 to 1997, Clim. Res., 15, 161–183, 2000. 4122

Knorr, W.: Annual and interannual CO_2 exchanges of the terrestrial biosphere: process based simulations and uncertainties, Global Ecol. Biogeogr., 9, 225–252, 2000. 4122

Knyazikhin, Y., Glassy, J., Privette, J. L., Tian, Y., Lotsch, A., Zhang, Y., Wang, Y., Morisette, J. T., Votava, P., Myeni, R. B., Nemani, R. R., and Running, S. W.: MODIS leaf area index (LAI) and fraction of photosynthetically active radiation absorbed by vegetation (FPAR) product (MOD15) algorithm theoretical basis document, 1999. 4124

Levin, I. and Kastens, U.: Inferring high-resolution fossil fuel CO_2 records at continental sites from combined $^{14}CO_2$ and CO observations, Tellus B, 59, 2007. 4133

Olivier, J. G. J., Van Aardenne, J. A., Dentener, F., Ganzeveld, L., and Peters, J. A. H. W.: Recent trends in global greenhouse gas emissions: regional trends and spatial distribution of key sources, in: Non-CO_2 Greenhouse Gases (NCGG-4), edited by: van Amstel, A., 325–330, Millpress, Rotterdam, The Netherlands, 2005. 4123

Pieterse, G., Bleeker, A., Vermeulen, A. T., Wu, Y., and Erisman, J. W.: High resolution modeling of atmosphere-canopy exchange of acidifying and eutrophying components and carbon dioxide for european forests, Tellus B, 59(3), 412–424, 2007. 4118, 4120, 4122

Randall, D. A., Wood, R. A., Bony, S., Colman, R., Fichefet, T., Fyfe, J., Kattsov, V., Pitman, A., Shukla, J., Srinivasan, J., Stouffer, R. J., Sumi, A., and Taylor K. E.: Climate models and their evaluation, in: Climate Change 2007: The Physical Science Basis. Contribution of working Group I to the Fourth Assessment Report of the Intergovernmental Panel on Climate Change, edited by: Solomon, S., Qin,D., Manning, M., Chen, Z., Marquis, M., Averyt, K., Tignor, M., and Miller, H., Cambridge University Press, Cambridge, United Kingdom and New York, 2007. 4118

Sellers, P. J., Randall, D. A., Collatz, G. J., Berry, J. A., Field, C. B., Dazlich, D. A., Zhang, C., Collelo, G. D., and Bounoua, L.: A revised land surface parameterization (SiB2) for atmospheric GCMs, Part I: Model formulation, J. Clim., 9, 676–705, 1996. 4118, 4121, 4122

Stohl, A. and Seibert, P.: Accuracy of trajectories as determined from the conservation of meteorological tracers, Q. J. Roy. Meteor. Soc., 124, 1465–1484, 1998. 4123

Stohl, A., Wotawa, G., Seibert, P., and Kromp-Kolb, H.: Interpolation errors in wind fields as a function of spatial and temporal resolution and their impact on different types of kinematic trajectories, J. Appl. Meteorol., 34, 2149–2165, 1995. 4123

Takahashi, T., Sutherland, S. C., Sweeney, C., Poisson, A., Metzl, N., Tillbrook, B., Bates, N., Wanninkhof, R., Feely, R. A., Sabine, C., Olafsson, J., and Nojiri, Y.: Global sea-air CO_2 flux based on climatological surface ocean pCO_2, and seasonal biological and temperature effects, Deep-Sea Res. II, 49, 1601–1622, 2002. 4123

Teillet, P. M., El Saleous, N., and Hansen, M.: An evaluation of the global 1-Km AVHRR land dataset, Int. J. Remote Sens., 21, 1987-2021, 2000. 4125

Ulden, A. P. v. and Wieringa, J.: Atmospheric boundary layer research at Cabauw, Bound.-Lay. Meteorol., 78, 39–69, 1996. 4126

Vermeulen, A. T., Eisma, R., Hensen, A., and Slanina, J.: Transport model calculations of nw

european methane emissions, Environ. Sci. Pollut., 2, 315–324, 1999. 4120, 4123
Vermeulen, A. T., Pieterse, G., Hensen, A., van den Bulk, W. C. M., and Erisman, J. W.: Comet: a lagrangian transport model for greenhouse gas emission estimation forward model technique and performance for methane, Atmos. Chem. Phys. Discuss., 6, 8727–8779, 2006, http://www.atmos-chem-phys-discuss.net/6/8727/2006/. 4118, 4120, 4123
Vidale, P. L. and Stoekli, R.: Prognostic canopy air space solutions for land surface exchanges, Theor. Appl. Climatol., 80, 245–257, 2005. 4122
World Meteorological Organisation: WMO WDCGC data summary, volume IV – Greenhouse gases and other atmospheric gases, Japan meteorological agency in cooperation with WMO, 31st edition, 2007. 4119
Wu, Y., Brashers, B., Finkelstein, P. L., and Pleim, J. E.: A multilayer biochemical dry deposition model – 1. model formulation, J. Geophys. Res., 108(D1), 4013–4013, 2003. 4121

Table 1. Description of the six cases considered for the model-to-measurement comparison.

Case number	Used data set
1	Takahashi
	Edgar Fast Track
2 or 5	Takahashi
	Edgar Fast Track
	FACEM GPP or SiB3 GPP
3	Takahashi
	Edgar Fast Track
	FACEM NPP
4 or 6	Takahashi
	Edgar Fast Track
	FACEM NEP or SiB3 NEP

Table 2. Description of the three European sites considered in the combined COMET and biospheric model framework.

Site name	Longitude [°]	Latitude [°]	Height(s) [m]	Description
Cabauw	4.93	51.97	20, 60, 120, 200	Continental
Hegyhatsal	16.65	46.97	10, 48, 82, 115	Deep continental
Mace Head	−9.54	53.20	26	Continental boundary

Table 3. Model performance for the prediction of CO_2 concentrations at the Cabauw tall tower site, using different data sets for source and sink strength estimates, see Table 1.

	R^2 [–]	σ [ppm]	Bias [ppm]
Measurements	–	17.1	–
Measurements (daytime)	–	12.9	–
Measurements (nighttime)	–	17.6	–
Case 1	0.63	10.0	−7.8
Case 2	0.35	11.4	−12.9
Case 3	0.62	13.7	−7.0
Case 4	0.67	16.7	−1.2
Case 4 (daytime)	0.75	14.0	0.5
Case 4 (nighttime)	0.57	17.2	−2.4
Case 5	0.41	10.6	−14.2
Case 6	0.69	15.1	−3.9
Case 6 (daytime)	0.74	12.0	−2.2
Case 6 (nighttime)	0.60	15.7	−4.9

Table 4. Model performance for the prediction of CO_2 concentrations at the Hegyhatsal Tall tower site, using different data sets for source and sink strength estimates, see Table 1.

	R^2 [–]	σ [ppm]	Bias [ppm]
Measurements	–	12.8	–
Measurements (daytime)	–	11.7	–
Measurements (nighttime)	–	12.6	–
Case 1	0.15	4.1	−11.0
Case 2	0.07	10.9	−18.5
Case 3	0.45	8.1	−9.9
Case 4	0.54	9.5	−4.7
Case 4 (daytime)	0.62	8.5	−4.0
Case 4 (nighttime)	0.46	9.2	−5.1
Case 5	0.04	10.8	−20.2
Case 6	0.44	23.1	3.5
Case 6 (daytime)	0.57	9.4	−2.7
Case 6 (nighttime)	0.40	25.8	8.8

Table 5. Model performance for the prediction of CO_2 concentrations at the site at Mace Head, using different data sets for source and sink strength estimates, see Table 1.

	R^2 [–]	σ [ppm]	Bias [ppm]
Measurements	–	5.9	–
Measurements (daytime)	–	5.7	–
Measurements (nighttime)	–	5.8	–
Case 1	0.45	4.4	−3.1
Case 2	0.29	5.6	−3.9
Case 3	0.52	5.0	−2.8
Case 4	0.54	6.1	−1.6
Case 4 (daytime)	0.62	5.7	−1.5
Case 4 (nighttime)	0.49	6.4	−1.7
Case 5	0.12	7.4	−4.9
Case 6	0.27	9.1	−0.8
Case 6 (daytime)	0.21	6.9	−1.8
Case 6 (nighttime)	0.44	10.2	0.0

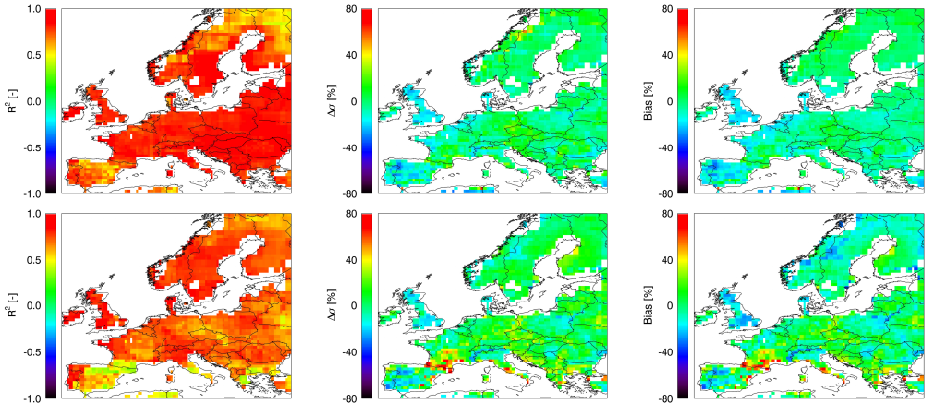

Fig. 1. The correlation (R^2), relative difference in the standard deviation ($\Delta\sigma$) and relative bias between the modelled FACEM and SiB3 GPP fluxes for the spring **(a)–(c)** and summer **(d)–(f)** season.

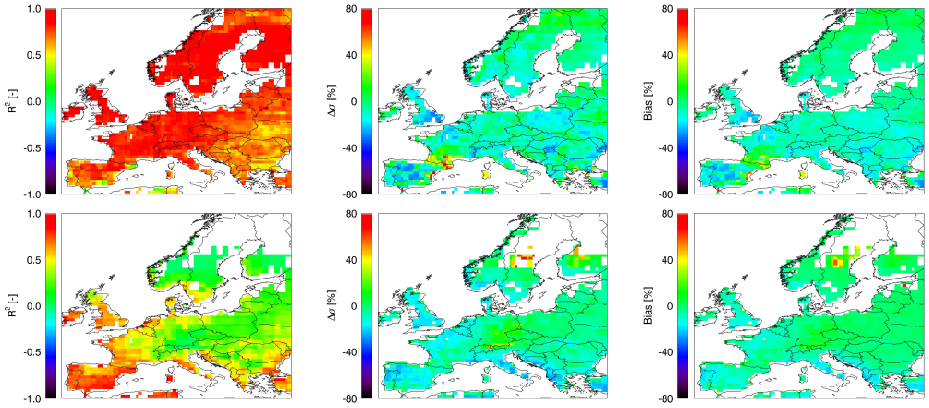

Fig. 1. Continued. The correlation (R^2), relative difference in the standard deviation ($\Delta\sigma$) and relative bias between the modelled FACEM and SiB3 GPP fluxes for the autumn **(g)–(i)** and winter **(j)–(l)** season.

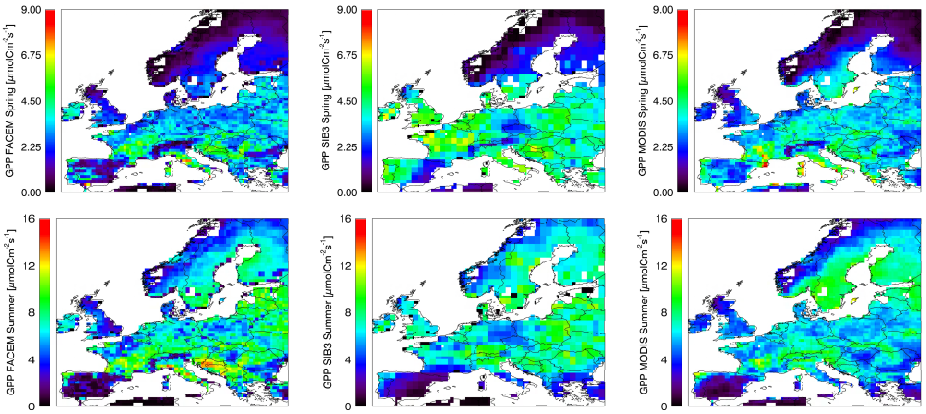

Fig. 2. Comparison of monthly averaged GPP with MODIS GPP for the Spring **(a)–(c)** and Summer **(d)–(f)** season.

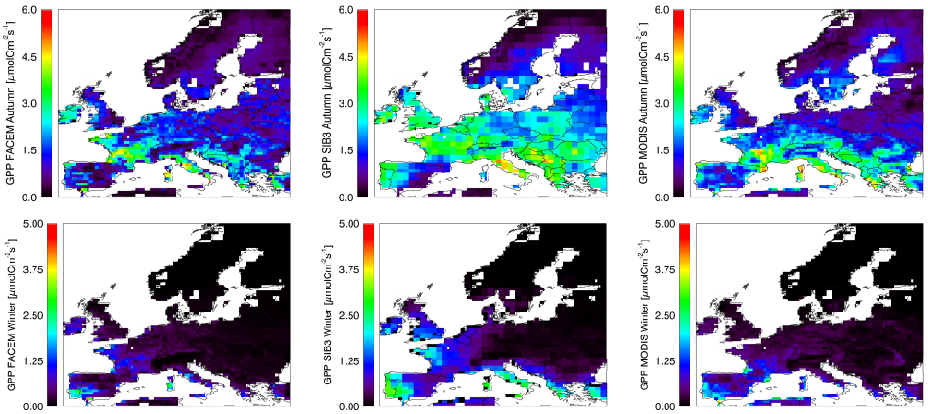

Fig. 2. Continued. Comparison of monthly averaged GPP with MODIS GPP for the Autumn **(g)–(i)** and Winter **(j)–(l)** season.

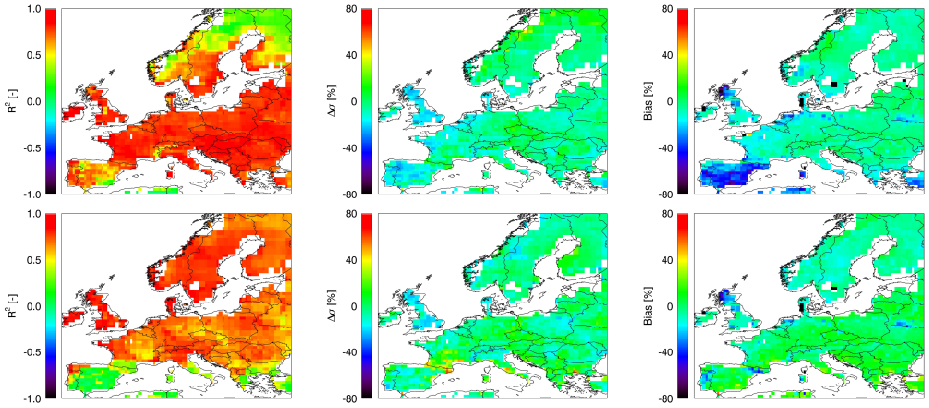

Fig. 3. The correlation (R^2), relative difference in the standard deviation ($\Delta\sigma$) and relative bias between the modelled FACEM and SiB3 NEP fluxes for the Spring **(a)–(c)**, Summer **(d)–(f)** season.

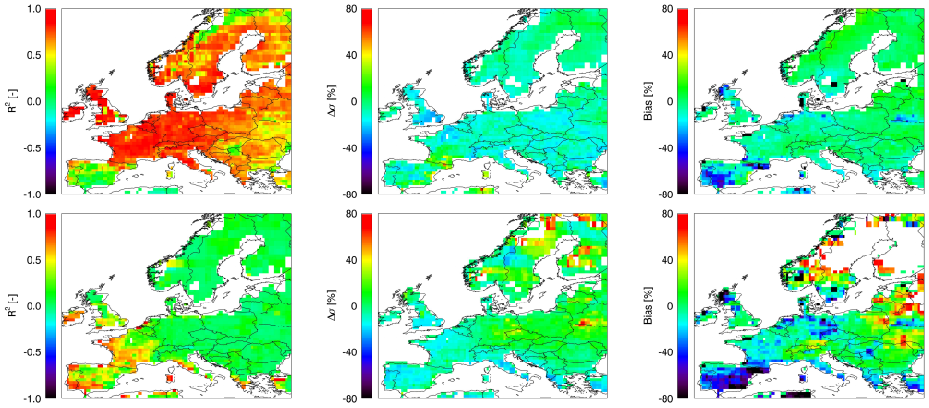

Fig. 3. Continued. The correlation (R^2), relative difference in the standard deviation ($\Delta\sigma$) and relative bias between the modelled FACEM and SiB3 NEP fluxes for the Autumn **(g)–(i)** and Winter **(j)–(l)** season.

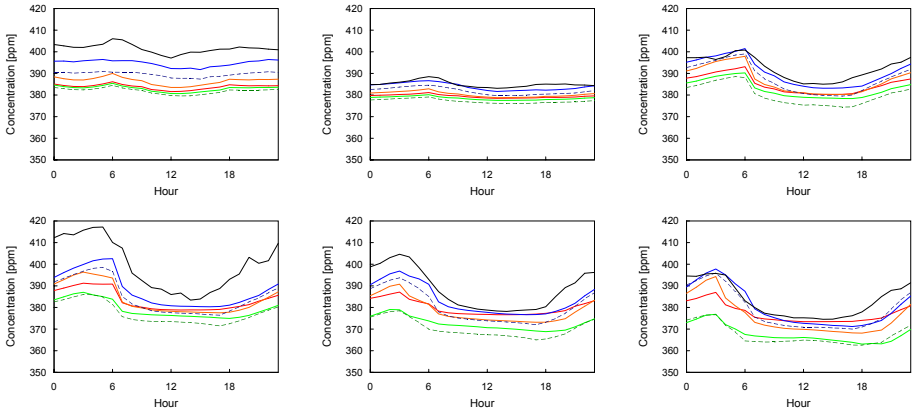

Fig. 4. The monthly averaged diurnal cycles of the modelled and measured signals at Cabauw for January **(a)** to June **(f)**: (black) measurements, (red) anthropogenic and oceanic estimates, (green) anthropogenic, oceanic and FACEM GPP estimates, (orange) anthropogenic, oceanic and FACEM NPP estimates, (blue) anthropogenic, oceanic and FACEM NEP estimates, (dashed green) anthropogenic, oceanic and SIB3 GPP estimates, (dashed blue) anthropogenic, oceanic and SIB3 NEP estimates.

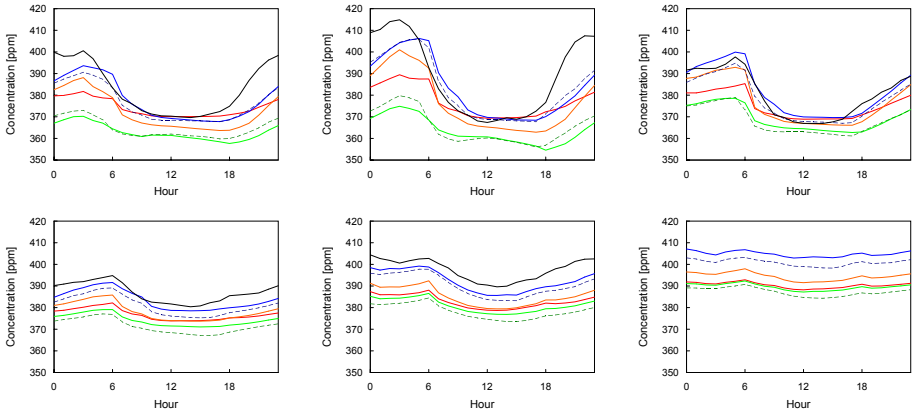

Fig. 4. Continued. The monthly averaged diurnal cycles of the modelled and measured signals at Cabauw for July **(g)** to December **(l)**: (black) measurements, (red) anthropogenic and oceanic estimates, (green) anthropogenic, oceanic and FACEM GPP estimates, (orange) anthropogenic, oceanic and FACEM NPP estimates, (blue) anthropogenic, oceanic and FACEM NEP estimates, (dashed green) anthropogenic, oceanic and SIB3 GPP estimates, (dashed blue) anthropogenic, oceanic and SIB3 NEP estimates.

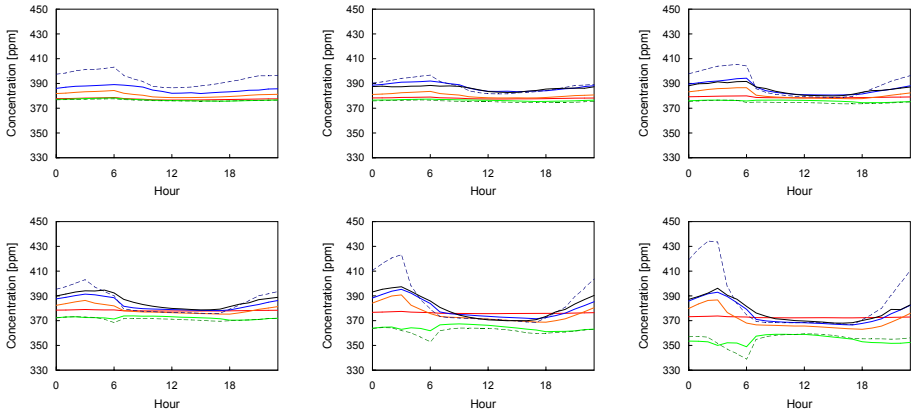

Fig. 5. The monthly averaged diurnal cycles of the modelled and measured signals at Hegyhatsal for January **(a)** to June **(f)**: (black) measurements, (red) anthropogenic and oceanic estimates, (green) anthropogenic, oceanic and FACEM GPP estimates, (orange) anthropogenic, oceanic and FACEM NPP estimates, (blue) anthropogenic, oceanic and FACEM NEP estimates, (dashed green) anthropogenic, oceanic and SIB3 GPP estimates, (dashed blue) anthropogenic, oceanic and SIB3 NEP estimates.

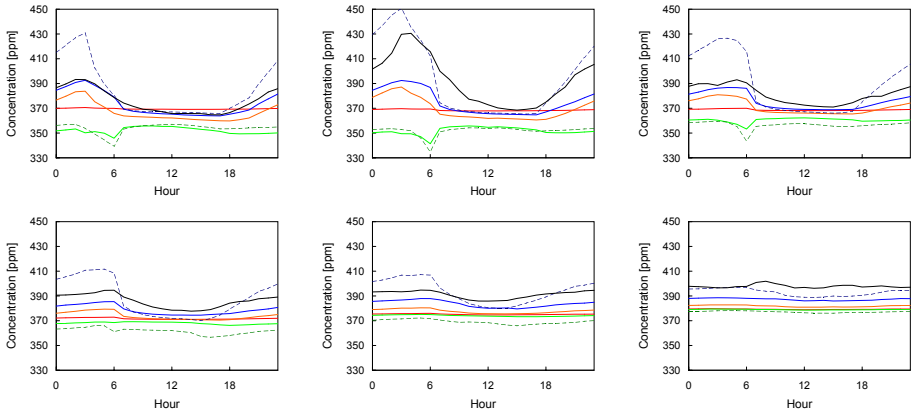

Fig. 5. Continued. The monthly averaged diurnal cycles of the modelled and measured signals at Hegyhatsal for July **(g)** to December **(l)**: (black) measurements, (red) anthropogenic and oceanic estimates, (green) anthropogenic, oceanic and FACEM GPP estimates, (orange) anthropogenic, oceanic and FACEM NPP estimates, (blue) anthropogenic, oceanic and FACEM NEP estimates, (dashed green) anthropogenic, oceanic and SIB3 GPP estimates, (dashed blue) anthropogenic, oceanic and SIB3 NEP estimates.

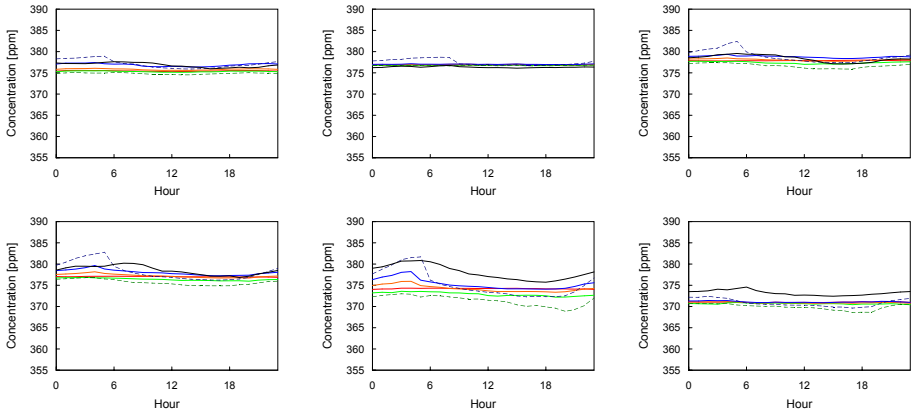

Fig. 6. The monthly averaged diurnal cycles of the modelled and measured signals at Mace Head for January **(a)** to June **(f)**: (black) measurements, (red) anthropogenic and oceanic estimates, (green) anthropogenic, oceanic and FACEM GPP estimates, (orange) anthropogenic, oceanic and FACEM NPP estimates, (blue) anthropogenic, oceanic and FACEM NEP estimates, (dashed green) anthropogenic, oceanic and SIB3 GPP estimates, (dashed blue) anthropogenic, oceanic and SIB3 NEP estimates.

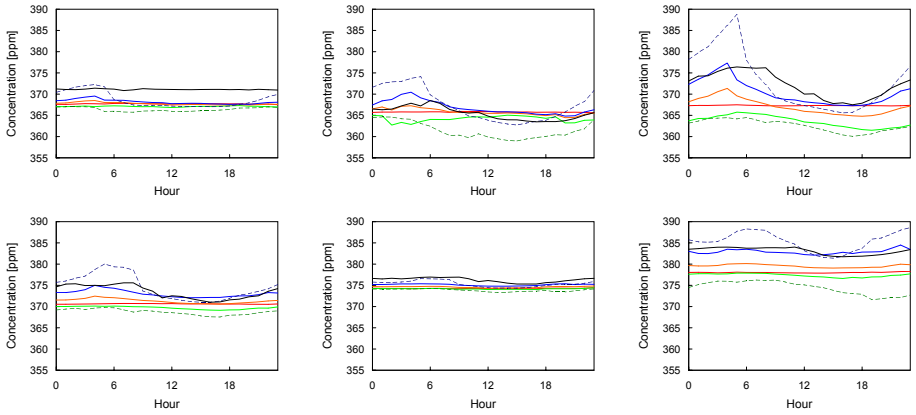

Fig. 6. Continued. The monthly averaged diurnal cycles of the modelled and measured signals at Mace Head for July **(g)** to December **(l)**: (black) measurements, (red) anthropogenic and oceanic estimates, (green) anthropogenic, oceanic and FACEM GPP estimates, (orange) anthropogenic, oceanic and FACEM NPP estimates, (blue) anthropogenic, oceanic and FACEM NEP estimates, (dashed green) anthropogenic, oceanic and SIB3 GPP estimates, (dashed blue) anthropogenic, oceanic and SIB3 NEP estimates.